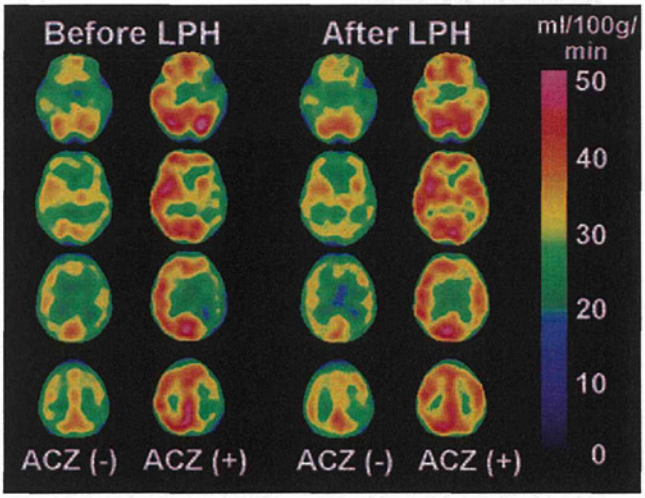

Fig. 5. Brain perfusion SPECT images of patient 3 exhibiting a reduction from 150 to 137 mm Hg in systolic blood pressure and from 94 to 79 mm Hg in diastolic blood pressure at 12 weeks after initiating the administration of LPH. CBF is slightly reduced, and CVR to acetazolamide (ACZ) is moderately reduced in the left MCA territory before LPH. While CBF remains unchanged after LPH, CVR to ACZ has improved in that region.

LPH to such patients, with average reductions of 11 mm Hg for systolic blood pressure and 10 mm Hg for diastolic blood pressure. The observations are consistent with those from a previous study [18].

While in the present study CBF did not differ between measurements before and after the administration of LPH, CVR significantly increased after the administration of LPH; 5 of the 18 patients were rated as having improved CVR, and none of the patients were rated as having deteriorated CVR. These data suggest that blood pressure-lowering therapy with LPH does apparently not result in worsening of cerebral hemodynamics within 3 months after the initiating the administration of LPH in patients with both hypertension and cerebral hemodynamic impairment due to symptomatic chronic ICA or MCA steno-occlusive disease. CVR often spontaneously improves in patients with major cerebral artery steno-occlusive disease, predominantly during the first few months after the onset of ischemic symptoms, provided no interval stroke occurs [10, 19]. This improvement is probably dependent on the development of collateral circulation [10]. The present study also showed that none of the variables, including the difference in blood pressure, were significantly associated with improved CVR. However, the absence of associations may be due to the small sample size.

In the present study, CBF and CVR did not differ between measurements taken before and after the administration of LPH in the hemisphere contralateral to the steno-occlusive artery, and all patients studied were rated as having unchanged CBF and CVR in the hemispheres. As these patients had normal CBF and CVR before the administration of LPH, the present data suggest that LPH does apparently not influence normal brain perfusion.

The present study has several limitations that require discussion. First, although the present study was an exploratory trial, statistical analysis power may be hampered by the small sample size. This is the most serious limitation. Although the prevalence of risk factors was quite different between patients with improved and unchanged CVR, no analysis was performed for statistical significance. Thus, the results of the present study are only preliminary and require confirmation in studies with larger populations. Second, patients did not receive any antihypertensive drugs within the 8 weeks after the last cerebral ischemic event and received LPH at 14 weeks after the last cerebral ischemic event. Further, only patients with moderately reduced CVR due to unilateral ICA or MCA steno-occlusive disease were enrolled in this study. Thus, the effect of LPH in an earlier phase after a cerebral ischemic event or in patients with severely reduced CVR or bilateral lesions remains unknown. Third, patients in the present study were examined for only 12 weeks after initiating the administration of LPH and for only 26 weeks after the last cerebral ischemic event. However, recurrent strokes in patients with hemodynamically compromised hemispheres generally occur during the first 6 months after the onset of ischemic symptoms [10, 19, 20]. Thus, the follow-up period in the present study may be long enough for examining the effect of LPH on brain perfusion. Finally, the comparator groups in this study may be suboptimal: confirmation of these results within a double-blind study of angiotensin receptor blocker plus thiazide diuretics versus only angiotensin receptor blocker would be of benefit.

Conclusions

Although the present study was exploratory and its results were preliminary due to the small sample size, the current data suggest that blood pressure-lowering therapy with LPH does apparently not result in worsening of cerebral hemodynamics in patients with both hyperten-

sion and cerebral hemodynamic impairment due to symptomatic chronic ICA or MCA steno-occlusive disease. Further study with larger sample sizes is needed to confirm this finding and to determine the effect of blood pressure-lowering therapy with LPH on the incidence of recurrent ischemic stroke.

Disclosure Statement

The authors declare that they have no conflict of interest to disclose.

References

1 Chobanian AV, Bakris GL, Black HR, Cushman WC, Green LA, Izzo JL Jr, Jones DW, Materson BJ, Oparil S, Wright JT Jr, Roccella EJ; the National High Blood Pressure Education Program Coordinating Committee: Seventh report of the joint national committee on prevention, detection, evaluation, and treatment of high blood pressure. Hypertension 2003;42:1206–1252.

2 Nishimura Y, Ito T, Saavedra JM: Angiotensin II AT_1 blockade normalizes cerebrovascular autoregulation and reduces cerebral ischemia in spontaneously hypertensive rats. Stroke 2000;31:2478–2486.

3 Moriwaki H, Uno H, Nagakane Y, Hayashida K, Miyashita K, Naritomi H: Losartan, an angiotensin II (AT_1) receptor antagonist, preserves cerebral blood flow in hypertensive patients with a history of stroke. J Hum Hypertens 2004;18:693–699.

4 Shah S, Khatri I, Freis ED: Mechanism of antihypertensive effects of thiazide diuretics. Am Heart J1978;95:611–618.

5 Stoltz JF, Zannad F, Kdher Y, Le Bray Des Boses B, Ghawi RE, Meilhac B, Cauchois G, Gentils M, Muller S: Influence of a calcium antagonist on blood rheology and arterial compliance in hypertension: comparison with a thiazide diuretic. Clin Hemorheol Microcirc 1999;21:201–208.

6 Araoye MA, Chang MY, Khatri IM, Freis ED: Furosemide compared with hydrochlorothiazide; long-term treatment of hypertension. JAMA 1978;240:1863–1866.

7 Calvo C, Gude F, Abellan J, Olivan J, Olmos M, Pita L, Sanz D, Sarasa J, Bueno J, Herrera J, Macias J, Sagastagoitia T, Ferro B, Vega A, Martinez J: A comparative evaluation of amlodipine and hydrochlorothiazide as monotherapy in the treatment of isolated systolic hypertension in the elderly. Clin Drug Invest 2000;19:317–326.

8 Zannad F, Bray-Desboscs L, el Ghawi R, Donner M, Thibout E, Stoltz JF: Effects of lisinopril and hydrochlorothiazide on platelet function and blood rheology in essential hypertension: a randomly allocated double-blind study. J Hypertens 1993;11:559–564.

9 Powers WJ: Cerebral hemodynamics in ischemic cerebrovascular disease. Ann Neurol 1991;29:231–240.

10 Ogasawara K, Ogawa A, Yoshimoto T: Cerebrovascular reactivity to acetazolamide and outcome in patients with symptomatic internal carotid or middle cerebral artery occlusion: a xenon-133 single-photon emission computed tomography study. Stroke 2002; 33:1857–1862.

11 Kuroda S, Houkin K, Kamiyama H, Mitsumori K, Iwasaki Y, Abe H: Long-term prognosis of medically treated patients with internal carotid or middle cerebral artery occlusion: can acetazolamide test predict it? Stroke 2001;32:2110–2116.

12 Ogasawara K, Ito H, Sasoh M, Okuguchi, Kobayashi M, Yukawa H, Terasaki K, Ogawa A: Quantitative measurement of regional cerebrovascular reactivity to acetazolamide using [^{123}I]iodoamphetamine autoradiographic method with single photon emission computed tomography: validation study using [^{15}O] H_2O positron emission tomography. J Nucl Med 2003;44:520–525.

13 Iida H, Itoh H, Nakazawa M, Hatazawa J, Nishimura H, Onishi Y, Uemura K: Quantitative mapping of regional cerebral blood flow using iodine-123-IMP and SPECT. J Nucl Med 1994;35:2019–2030.

14 Friston KJ, Frith CD, Liddle PF, Dolan RJ, Lammertsma AA, Frackowiak RS: The relationship between global and local changes in PET scans. J Cereb Blood Flow Metab 1990; 10:458–466.

15 Takeuchi R, Matsuda H, Yoshioka K, Yonekura Y: Cerebral blood flow SPET in transient global amnesia with automated ROI analysis by 3DSRT. Eur J Nucl Med Mol Imaging 2004;31:578–589.

16 Brenner BM, Cooper ME, de Zeeuw D, Keane WF, Mitch WE, Parving HH, Remuzzi G, Snapinn SM, Zhang Z, Shahinfar S; RENAAL Study Investigators: Effects of losartan on renal and cardiovascular outcomes in patients with type 2 diabetes and nephropathy. N Engl J Med 2001;345:861–869.

17 Dahlöf B, Devereux RB, Kjeldsen SE, Julius S, Beevers G, de Faire U, Fyhrquist F, Ibsen H, Kristiansson K, Lederballe-Pedersen O, Lindholm LH, Nieminen MS, Omvik P, Oparil S, Wedel H; LIFE Study Group: Cardiovascular morbidity and mortality in the Losartan Intervention For Endpoint reduction in hypertension study (LIFE): a randomised trial against atenolol. Lancet 2002; 359:995–1003.

18 Ruilope LM, Simpson RL, Toh J, Arcuri KE, Goldberg AI, Sweet CS: Controlled trial of losartan given concomitantly with different doses of hydrochlorothiazide in hypertensive patients. Blood Press 1996;5:32–40.

19 Widder B, Kleiser B, Krapf H: Course of cerebrovascular reactivity in patients with carotid artery occlusions. Stroke 1994;25:1963–1967.

20 Webster MW, Makaroun MS, Steed DL, Smith HA, Johnson DW, Yonas H: Compromised cerebral blood flow reactivity is a predictor of stroke in patients with symptomatic carotid artery occlusive disease. J Vasc Surg 1995;21:338–345.

J Neurol (2012) 259:1698–1705
DOI 10.1007/s00415-011-6402-5

ORIGINAL COMMUNICATION

Fractional anisotropy in the centrum semiovale as a quantitative indicator of cerebral white matter damage in the subacute phase in patients with carbon monoxide poisoning: correlation with the concentration of myelin basic protein in cerebrospinal fluid

Takaaki Beppu · Shunrou Fujiwara · Hideaki Nishimoto · Atsuhiko Koeda · Shinsuke Narumi · Kiyoshi Mori · Kuniaki Ogasawara · Makoto Sasaki

Received: 23 October 2011 / Accepted: 26 December 2011 / Published online: 19 January 2012

Abstract Carbon monoxide (CO) poisoning leads to demyelination of cerebral white matter (CWM) fibers, causing chronic neuropsychiatric symptoms. To clarify whether fractional anisotropy (FA) from diffusion tensor imaging in the centrum semiovale can depict demyelination in the CWM during the subacute phase after CO inhalation, we examined correlations between FA in the centrum semiovale and myelin basic protein (MBP) in cerebrospinal fluid. Subjects comprised 26 adult CO-poisoned patients ≤60 years old. MBP concentration was examined for all patients at 2 weeks after CO inhalation. The mean FA of the centrum semiovale bilaterally at 2 weeks was also examined for all patients and 21 age-matched healthy volunteers as controls. After these examinations, the presence of chronic symptoms was checked at 6 weeks after CO poisoning. Seven patients displayed chronic symptoms, of whom six showed abnormal MBP concentrations. The remaining 19 patients presented no chronic symptoms and no abnormal MBP concentrations, with MBP concentrations undetectable in 16 patients. The MBP concentration differed significantly between patients with and without chronic symptoms. The mean FA was significantly lower in patients displaying chronic symptoms than in either patients without chronic symptoms or controls. After excluding the 16 patients with undetectable MBP concentrations, a significant correlation was identified between MBP concentration and FA in ten patients. The present results suggest that FA in the centrum semiovale offers a quantitative indicator of the extent of demyelination in damaged CWM during the subacute phase in CO-poisoned patients.

Keywords Carbon monoxide poisoning · Cerebral white matter fiber · Demyelination · Diffusion tensor imaging · Fractional anisotropy · Myelin basic protein

Abbreviation

CNS	Central nervous system
CSF	Cerebrospinal fluid
CO	Carbon monoxide
COHb	Carboxyhemoglobin
DNS	Delayed neuropsychiatric sequelae
DTI	Diffusion tensor imaging
FA	Fractional anisotropy
ADC	Apparent diffusion coefficient
GCS	Glasgow coma scale
MBP	Myelin basic protein

T. Beppu (✉) · S. Fujiwara · H. Nishimoto · K. Ogasawara
Department of Neurosurgery, Iwate Medical University, Uchimaru 19-1, Morioka 020-8505, Japan
e-mail: tbeppu@iwate-med.ac.jp

T. Beppu
Department of Hyperbaric Medicine, Iwate Medical University, Uchimaru 19-1, Morioka 020-8505, Japan

A. Koeda
Department of Psychiatry, Iwate Medical University, Uchimaru 19-1, Morioka 020-8505, Japan

S. Narumi
Department of Neurology, Iwate Medical University, Uchimaru 19-1, Morioka 020-8505, Japan

K. Mori
Iwate Prefectural Advanced Critical Care and Emergency Center, Morioka, Japan

M. Sasaki
Advanced Medical Research Center, Iwate Medical University, Morioka, Japan

MRI Magnetic resonance imaging
ROI Region of interest
T2WI T2-weighted magnetic resonance imaging

Introduction

Approximately 30% of patients surviving acute carbon monoxide (CO) poisoning display various chronic neuropsychiatric symptoms [31, 32]. Of these, approximately two-thirds demonstrate persistent neurological symptoms from the acute phase to the chronic phase. The remaining one-third show delayed neuropsychiatric sequelae (DNS), which are recurrent neuropsychiatric symptoms occurring after an interval of apparent normality ("lucid interval;" mean duration 22 days) following apparent recovery from acute symptoms [6, 33]. Animal experiments and some clinical studies have led to the hypothesis that damage after CO poisoning results from complicated mechanisms due to CO-mediated toxicity: mitochondrial oxidative stress in the central nervous system (CNS) following CO-induced tissue hypoxia [35]; perivascular oxidative stress mediated by intravascular neutrophil activation [26]; and alteration of myelin basic protein (MBP), a major myelin component in the CNS, due to lipid peroxygenation leading to auto-immunological demyelination of CNS [24, 25]. Auto-immunological demyelination induces further inflammation in the cerebral white matter (CWM) [31]. Gray matter structures, such as the cerebral cortex, basal ganglia and hippocampus, must be damaged by severe hypoxia, since these structures display higher cellular activity and higher oxygen requirements than white matter structures and are more vulnerable to oxygen deprivation [29]. However, damage in the CWM is seen in patients both with and without damage to gray matter structures, and the severity of CWM damage appears to correlate with prognosis in CO-poisoned patients [15, 34].

Assessment of CWM damage caused by CO poisoning in the acute or subacute phase contributes to predictions of progress to DNS and prognosis of chronic symptoms, and appropriate triage of patients with CO poisoning for observation and treatment. Additional quantitative and objective examinations are desirable for assessment of CWM damage after CO poisoning. However, no universally accepted severity scale in routine examinations, such as level of consciousness or carboxyhemoglobin concentration, is available for assessing CWM damage caused by CO poisoning. This is because clinical features are largely affected by the degree of cellular hypoxia resulting from binding of CO to myoglobin rather than hemoglobin and may be markedly affected by various conditions before admission, such as the duration before hospitalization and the care provided before hospitalization [7, 12, 20]. As one of mechanisms for damage in CWM is auto-immunological demyelination, measuring the MBP concentration in the cerebrospinal fluid (CSF) has recently been proposed as an indicator for the extent of CWM damage after CO poisoning [11, 14]. However, detection of MBP using a lumbar tap is a highly invasive procedure and only indicates white-matter damage somewhere within the entire CNS. A less-invasive, objective and quantitative examination that could be used in place of measuring MBP is therefore desired. Diffusion tensor imaging (DTI), a magnetic resonance imaging (MRI) sequence, is potentially more sensitive for detecting demyelination in CWM. Among various quantitative parameters such as apparent diffusion coefficient (ADC) and eigenvalues derived from DTI, fractional anisotropy (FA) has been recognized as the most useful for evaluating the integrity of CWM fibers [2]. Indeed, FA is frequently used for evaluating the extent of damaged CWM fibers in patients with demyelinating diseases such as multiple sclerosis [1, 27]. CO poisoning causes damage in various regions of the CWM, but the centrum semiovale has been considered a region more responsible for chronic neuropsychiatric symptoms after CO poisoning than other regions [4, 10, 19, 22]. Herein, we measured FA from DTI at the centrum semiovale in CO-poisoned patients, and evaluated the correlation between the FA and concentration of MBP in the CSF. This study aimed to clarify whether FA in the centrum semiovale offers a quantitative indicator of the extent of demyelination in damaged CWM during the subacute phase in CO-poisoned patients.

Methods

Patients

All study protocols were approved by the Ethics Committee of Iwate Medical University, Morioka, Japan. Patients recruited to this study were admitted to Iwate Medical University Hospital between April 2008 and February 2011. Entry criteria for this study were: age $\geq$20 but $\leq$60 years in patients who had suffered from CO poisoning caused by a fire or charcoal burning; performance of DTI and measurement of MBP concentration according to the protocol in this study; no past history of brain disorders, including surgical operation, irradiation, stroke, infection or demyelinating disease; and provision of written informed consent to participate. Diagnosis was based on present history of exposure to CO and presence of acute neurological symptoms such as impairment of consciousness and headache on admission. After excluding patients

who did not meet the entry criteria, 26 patients were enrolled. Mean duration from the scene of CO exposure to arrival at our institute was 5.0 h (range 0.3–81 h). All patients were treated with hyperbaric oxygenation therapy (HBO_2) (60 min of 100% oxygen inhalation via mask at 2.8 atmospheres absolute) started within 24 h of admission. HBO_2 was continued with a single daily session for a week excluding the weekend. HBO_2 was further continued for 4–8 weeks in cases with persistent symptoms. If DNS occurred, HBO_2 was restarted and continued until 2 months after CO exposure. HBO_2 was discontinued upon patient request or when symptoms were sufficiently improved. Duration of HBO_2 administration for all patients ranged from 1 to 60 sessions (mean 12 sessions). The day of CO inhalation was defined as day 1 in this study.

Measurement of MBP concentration in CSF

MBP concentration in the CSF was examined using a lumbar tap at 2 weeks after CO poisoning (between day 12 and day 16) for all patients. Obtained CSF was frozen at −20°C within 1 h after lumbar tap, then the frozen CSF was transported on dry ice to an outside laboratory (SRL, Tokyo, Japan). MBP in the CSF was assayed and measured using a MBP ELISA kit (Cosmic Corp., Tokyo, Japan) immediately after arrival at the laboratory. If the assay was delayed for a long time, frozen CSF was stored at −80°C. An abnormal MBP concentration was defined as ≥102 pg/ml. When the level of MBP was below the limit of detection, the result from the laboratory was reported as MBP ≤40 pg/ml.

DTI

For all patients, DTI was also performed at 2 weeks (between day 12 and day 16) using a 3.0-T whole-body scanner (GE Yokogawa Medical Systems, Tokyo, Japan) and 8-channel coil. Measurements of FA and ADC were performed using data from DTI (repetition time, 10,000 ms; echo time, 62 ms; matrix 128 × 128; field of view, 240 × 240 mm; 4 mm thickness with 1.5 mm gap; 6 motion-probing gradient directions; b value, 1,000 s/mm^2). The region of interest (ROI) was manually placed in the bilateral centrums semiovale in the CWM on non-diffusion-weighted images (Fig. 1). FA and ADC were measured bilaterally at the centrum semiovale, using free MRIcro software (http://www.cabiatl.com/mricro/). The FA and ADC for each subject were determined as the mean of values measured twice by the same investigator (S.F.), who was blinded to clinical data. The second measurement was performed 1 week after the first test, using a different randomized order of measurements from the first test.

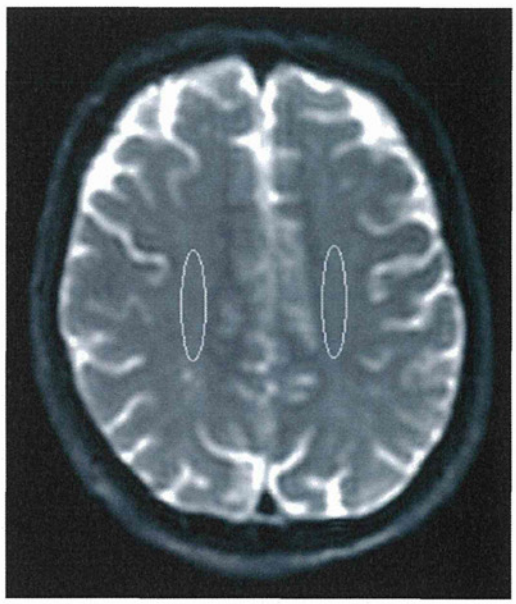

Fig. 1 Measurements of FA and ADC value at the centrum semiovale in a patient (case 7 in group S). Regions of interest (ROIs) were placed bilaterally on the centrum semiovale in non-diffusion-weighted image

Finally, the mean FA and mean ADC values for the right and left centrum semiovale were calculated and defined as absolute values for each subject. The same procedures described above were performed for 21 age-matched healthy volunteers as controls (18 men, 3 women; mean age 41 ± 10 years, range 22–56 years).

Observation of symptoms

Neurological symptoms were continuously observed for 6 weeks after admission using routine neurological examinations. Patients were assigned to one of two groups according to clinical behavior at 6 weeks (day 40–44) after CO poisoning: group S, patients displaying neuropsychiatric symptoms; group A, patients showing asymptomatic status. Group S included both patients with symptoms persisting for 6 weeks and patients with DNS. DNS was defined as recurrent symptoms after apparent improvement of acute symptoms followed by a lucid interval. General intellectual function was also estimated using the mini-mental state examination (MMSE) [9] at 6 weeks after CO exposure. We defined the normal range, borderline range and dementia according to MMSE scores as ≥27, ≤26 but ≥22, and ≤21, respectively. When scores were considered borderline, patients with educational background ≥9 years and evidence of obvious personality change according to interviews with family members were diagnosed with dementia.

Statistical analyses

We statistically compared differences in mean age among group S, group A and controls using the Mann-Whitney U test. The incidence of abnormal ($\geq$102 pg/ml) MBP concentration was compared between the two patient groups (group S and group A) using the χ^2 for independence test. Mean FA and mean ADC values among two patients groups and controls were compared using the Mann-Whitney U test. Intra-operator reliability for all absolute FA and ADC values was evaluated according to classification of the intra-class correlation coefficient (ICC) [21]. For ICC(1,1) and ICC(1,k) as intra-operator reliability, agreement of all absolute values between the first and second tests was analyzed for right and left lesions using one-factor analysis of variance. After excluding patients showing undetectable concentrations of MBP ($\leq$40 pg/ml), the correlation between MBP and mean FA value was estimated using Spearman's correlation coefficient by rank test. Statistical significance was established at the $p < 0.05$ level in all analyses.

Results

A total of 51 patients were admitted to our institute for treatment of CO poisoning between April 2008 and February 2011. After excluding 25 patients who did not meet the entry criteria for this study, a total of 26 patients (24 men, 2 women; mean age 40.1 $\pm$ 11.4 years) were enrolled. All patient data are summarized in Table 1. In 19 (73%) of 26 patients, acute symptoms resolved completely within 4 days after admission, and no neuropsychiatric symptoms were present at 6 weeks from CO-inhalation (group A). The remaining seven patients (27%) displayed chronic neuropsychiatric symptoms at 6 weeks (group S), including four patients with continuous persistence of symptoms for 6 weeks and three patients exhibiting DNS

Table 1 Summary of all patients

Case	Group	Age	Etiology	COHb (%)	GCS	MBP (pg/ml)	Mean FA	Mean ADC	Main symptom at 6 weeks	MMSE score
1	S	29	Suicide	24.8	11	252	0.345	0.622	Dementia (persistent)	23
2	S	57	Suicide	25.1	10	176	0.344	0.548	Parkinsonism (persistent)	27
3	S	38	Suicide	1.5	6	468	0.239	0.494	Apallic syndrome (persistent)	NS
4	S	55	Suicide	39.7	3	376	0.346	0.548	Dementia (persistent)	16
5	S	56	Suicide	13.5	11	130	0.338	0.584	Akinetic mutism (DNS)	NS
6	S	29	Suicide	3.6	14	99	0.353	0.498	Parkinsonism (DNS)	28
7	S	48	Suicide	28.6	6	110	0.317	0.565	Dementia (DNS)	23
1	A	22	Suicide	20.5	15	52.8	0.488	0.492	None	29
2	A	31	Suicide	47.3	13	40.6	0.354	0.494	None	30
3	A	22	Suicide	9.3	12	63.6	0.447	0.555	None	30
4	A	47	Heating	33.3	14	$\leq$40	0.441	0.496	None	30
5	A	44	Heating	13.7	15	$\leq$40	0.388	0.528	None	30
6	A	26	Suicide	1.9	15	$\leq$40	0.395	0.504	None	30
7	A	47	Heating	22.6	14	$\leq$40	0.393	0.551	None	29
8	A	28	Suicide	19.2	15	$\leq$40	0.440	0.521	None	30
9	A	41	Suicide	2.7	11	$\leq$40	0.381	0.487	None	30
10	A	55	Heating	14.0	13	$\leq$40	0.366	0.504	None	30
11	A	35	Suicide	25.3	8	$\leq$40	0.425	0.497	None	30
12	A	56	Suicide	12.2	15	$\leq$40	0.395	0.501	None	30
13	A	36	Suicide	44.1	12	$\leq$40	0.398	0.513	None	30
14	A	34	Suicide	31.0	12	$\leq$40	0.394	0.530	None	30
15	A	57	Heating	40.1	13	$\leq$40	0.400	0.541	None	30
16	A	32	Suicide	19.3	10	$\leq$40	0.358	0.509	None	30
17	A	34	Suicide	38.6	5	$\leq$40	0.406	0.535	None	30
18	A	36	Suicide	23.5	10	$\leq$40	0.358	0.520	None	30
19	A	48	Suicide	44.0	6	$\leq$40	0.352	0.539	None	30

COHb and GCS indicate results of the initial examination

COHb carboxyhemoglobin, *GCS* Glasgow coma scale, *NS* no study performed because of unconsciousness

after apparent improvement of acute symptoms followed by a lucid interval. DNS in three patients occurred after DTI and measurement of MBP on day 21 in case 5, day 19 in case 6 and day 18 in case 7. Mean age was 45 ± 12 years in group S, 38 ± 11 years in group A and 41 ± 10 years in controls. No significant differences in age were found between groups S and A ($p = 0.24$), between group S and controls ($p = 0.51$), or between group A and controls ($p = 0.40$).

In the seven patients in sroup S, six showed abnormal MBP concentrations (≥102 pg/ml), and one patient showed a level of 99 pg/ml. None of the 19 patients in group A showed abnormal concentrations of MBP, with 16 patients showing undetectable concentrations of MBP (≤40 pg/ml). The incidence of an abnormal MBP levels was statistically different between groups P and A ($p < 0.001$). MBP concentrations for the four patients with persistent symptoms in group S, for the three patients with DNS in group S and for the three patients in group A were more than ≥150 pg/ml, around 100 pg/ml and around 50 pg/ml, respectively (Table 1).

Table 2 shows ranges and means of FA and ADC for each group. The range of FA for group S slightly overlapped that for group A, but differed markedly from that for controls. Ranges of FA for group A and controls were similar. The mean FA for group S was significantly lower than those for group A ($p < 0.001$) and controls ($p < 0.001$), whereas no significant difference was found between group A and controls ($p = 0.57$) (Fig. 2a). In Fig. 2a, individual mean FA values of the three patients with DNS were not obviously different from those of the four patients with persistent symptoms in group S. Group S patients were clearly differentiated from group A patients at a cutoff of 0.353 (100% sensitivity, 94.7% specificity) and from controls at a cutoff of 0.360 (100% sensitivity, 100% specificity). On the other hand, the range of ADC in each group was similar, and the mean ADC did not differ significantly among any of the three groups (Fig. 2b). Intra-operator reliability for absolute FA was classified as "almost perfect" for the centrum semiovale bilaterally; ICC(1,1) and ICC(1,*k*) were 0.88 and 0.93 for the right side, and 0.95 and 0.98 for the left side, respectively. Intra-operator reliability for absolute ADC was also classified as "almost perfect" for bilateral centrum semiovale; ICC(1,1) and ICC(1,*k*) were 0.98 and 0.99 for the right side, and 0.91 and 0.95 for the left side, respectively.

After excluding 16 patients showing undetectable levels (≤40 pg/ml), the ten remaining patients (all patients in groups S and 3 patients in group A) showed a strong correlation between the mean FA and MBP ($r = -0.79$, $p = 0.02$) (Fig. 3).

Discussion

Ide et al. [11] have documented that MBP concentration in patients with DNS showed marked elevation around 2 weeks after CO poisoning, peaking at around 30 days.

Table 2 Range and mean value of FA and ADC for each group

	FA		ADC ($\times 10^{-3}$ mm^2/s)	
	Range	Mean	Range	Mean
Group S	0.239–0.353	0.326 ± 0.040	0.494–0.622	0.551 ± 0.045
Group A	0.352–0.447	0.395 ± 0.029	0.487–0.601	0.517 ± 0.021
Controls	0.363–0.445	0.400 ± 0.027	0.472–0.580	0.517 ± 0.023

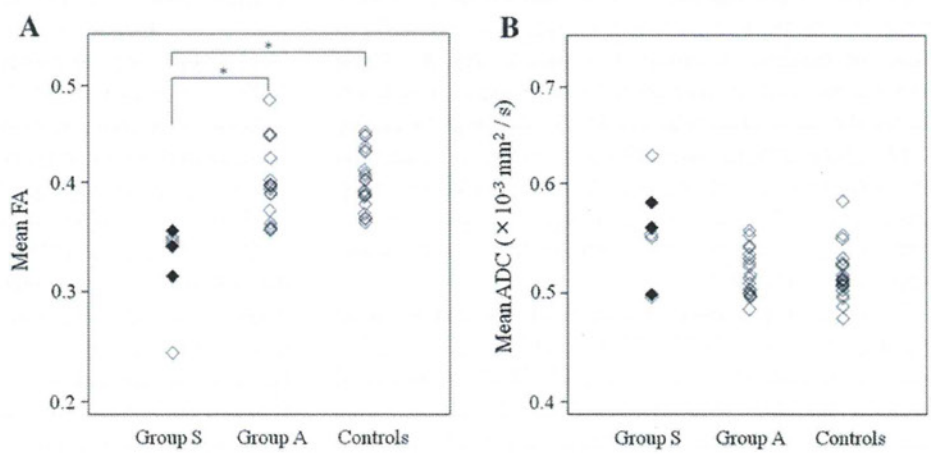

Fig. 2 Differences of mean FA (**a**) and mean ADC (**b**) values in the centrum semiovale bilaterally among group S, group A and controls. In group S, *black and white squares* represent patients with DNS and persistent symptoms, respectively (*$p < 0.001$).

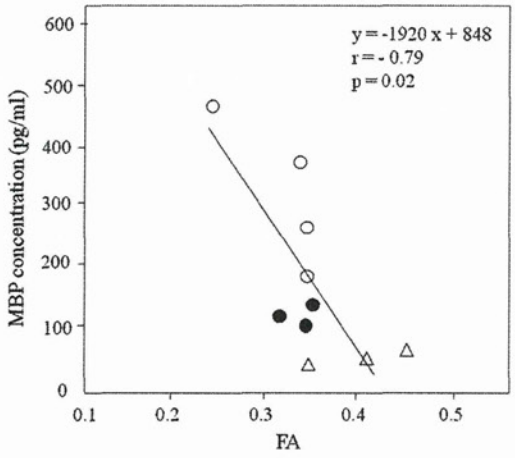

Fig. 3 Correlation between FA and MBP concentration in ten patients showing MBP concentration >40 pg/ml. *White circle*, patient with persistent chronic symptoms in group S; *black circle*, patient with DNS in group S; *triangle*, patient in group A

The timing for MBP measurements in the present study was thus established at 2 weeks (between day 12 and day 16) after admission. As a result, the incidence of abnormal MBP concentration was significantly higher in patients with chronic neuropsychiatry symptoms (group S) than in patients without chronic symptoms (group A) or controls. These results suggest that patients in group S certainly suffered from demyelinating changes somewhere in the CWM and support the theory that chronic neuropsychiatric symptoms after CO intoxication result from progressive demyelination in the CWM [24, 25]. The MBP concentration in case 6 was slightly lower (99 pg/ml) than the abnormal level, but the patient displayed akinetic mutism compatible with DNS at 1 week after measurement of MBP. The concentration of MBP in this patient might have been on the way to reaching abnormal levels, as demyelination of CWM in patients with DNS has been considered to undergo gradual progression during the lucid interval [13]. MBP concentrations of DNS patients were between those of patients with persistent symptoms in group S and those of patients in group A (Table 1; Fig. 3). These findings may indicate that demyelination begins to progress during the lucid interval before DNS. Although measuring MBP concentrations thus offers a useful indicator for assessing the extent of demyelination due to CO poisoning, detection of MBP using a lumbar tap is a highly invasive procedure and only indicates white-matter damage somewhere within the CNS.

Neuroimaging is minimally invasive and can visualize any region in the CWM. T2-weighted imaging (T2WI) often depicts abnormalities in the CWM in CO-poisoned patients. However, the interpretation of findings from routine MRI is difficult, as hyperintense foci in the CWM on T2WI can represent various progressive histological changes, including vasogenic edema, multiple necrosis, extensive axonal destruction and/or demyelination without axonal destruction [4, 12]. We therefore performed DTI in the same period as detection of MBP, since DTI is potentially more sensitive for assessing the extent of demyelinating changes in the CWM than other MRI sequences. As progressive reduction of FA values with age has been reported [5], we compared patients <60 years old with age-matched controls in this study. The finding of no significant difference in mean age among groups S, group A and controls suggests a negligible contribution of aging to FA values in this study. Previous reports have documented damage in various regions of the CWM after CO poisoning [8, 18, 28]. Indeed, some studies have reported correlations between FA values in various regions of the CWM in the chronic phase and cognitive dysfunction among CO-poisoned patients with DNS [16, 23, 30]. However, the centrum semiovale in the CWM has been suggested as a key region responsible for chronic neurological symptoms [4, 10, 19, 22]. A study using DTI at various phases after CO poisoning has also shown that FA in the centrum semiovale changes in parallel with cognitive impairments or neurological symptoms [17]. Based on these reports, we placed the ROI on the centrum semiovale to measure FA and ADC from DTI. As a result, mean FA for group S presenting with chronic neuropsychiatric symptoms was significantly lower than that for group A presenting with no chronic symptoms or that for controls consisting of healthy volunteers, whereas no significant difference was evident between group A and controls. In contrast, mean ADC did not differ significantly among the three groups. FA must be more sensitive for detecting CWM damage than ADC. Furthermore, these findings suggest that white matter fibers in the centrum semiovale were demyelinated in the subacute phase (2 weeks after poisoning) in CO-poisoned patients presenting with chronic symptoms. Notably, reductions in FA, suggestive of demyelination, were already present in the centrum semiovale before the recurrence of symptoms in the three patients with DNS. The reliability of this finding is supported by the result that MBP concentrations in DNS patients showed greater increases than those in group A patients at 2 weeks. These findings indicate the possibility of using FA in the centrum semiovale as an appropriate examination for predicting DNS during the lucid interval.

Our pilot study of DTI for CO-poisoned patients showed that FA enables representation of damage to white matter fibers in the centrum semiovale of patients with chronic neuropsychiatric symptoms [3]. That report, however, failed to demonstrate any correlation between FA in the centrum semiovale and MBP concentration, presumably because of the small sample size. Although subject criteria

were more strictly established in the present study than in our previous investigation, the greater number of subjects in this study allow us to show a linear correlation between FA and MBP in ten patients showing MBP concentrations >40 pg/ml. This finding validated the use of the centrum semiovale to represent various demyelinated lesions in the CWM, and FA in the centrum semiovale obviously offers a quantitative indicator of demyelination in CO-poisoned patients with chronic neuropsychiatric symptoms.

Some limitations must be considered in the interpretation of the study results. First, FA in the centrum semiovale may not strictly mirror the amount of demyelination in the whole CWM, although FA in the centrum semiovale correlated with MBP concentration. In group S, FA values in the centrum semiovale of the three DNS patients were not clearly different from those of the four patients with persistent symptoms (Fig. 2a), whereas MBP seemed to allow differentiation between subgroups in group S (around 100 pg/ml in patients with DNS and ≥150 pg/ml in patients with persistent chronic symptoms). This discrepancy might hypothetically be explained if demyelinated lesions in patients with persistent symptoms vary more than those in DNS patients. FA measured in this study suggests the magnitude of demyelination in the centrum semiovale, whereas MBP concentration not only indicates the magnitude, but also the width of demyelination in the whole CNS. We think that FA in the centrum semiovale cannot allow differentiation of the severity of CWM damage among subjects including patients with DNS and those with persistent symptoms. Second, the chronic neuropsychiatric symptoms seen after CO poisoning may not be solely attributable to demyelinating changes in fibers of the centrum semiovale. However, knowing to the focus on the region of the CWM is obviously very useful when evaluating the extent of CO-induced CWM damage using neuroimaging. We considered that the centrum semiovale represents the main region of damage and should be the focus of attention on neuroimaging in the subacute phase after CO poisoning [10]. Third, the sample size in this study was still small, with markedly fewer subjects in group S than in group A. The small number of DNS patients resulted in difficulties with statistical comparisons between subgroups in group S and other groups. However, the small sample size resulted from the strict entry criteria for this study. Furthermore, we did not select subjects with any bias other than the criteria established for this study. Indeed, percentages for patients with and without chronic symptoms in this study were in agreement with the results of previous reports [6, 33]. Fourth, findings in this study cannot be applied to patients over 60 years old. In senior patients, FA values may be overestimated as aging may lead to reduced FA values.

Conclusions

This is the first report to find that FA in the CWM correlates with MBP concentrations in the CSF during the subacute phase in CO-poisoned patients. The identification of a significant negative correlation between FA in the centrum semiovale and MBP concentration validates the concept that the centrum semiovale can reveal various demyelinated lesions in the CWM and that FA in the centrum semiovale offers a quantitative indicator of demyelination in CO-poisoned patients with chronic neuropsychiatric symptoms.

Acknowledgments This study was supported in part by a Grant-in-Aid for Scientific Research (C) and for the Strategic Medical Science Research Center for Advanced Medical Science Research from the Ministry of Science, Education, Sports and Culture, Japan.

Conflicts of interest None.

References

1. Bammer R, Augustin M, Strasser-Fuchs S, Seifert T, Kapeller P, Stollberger R, Ebner F, Hartung HP, Fazekas F (2000) Magnetic resonance diffusion tensor imaging for characterizing diffuse and focal white matter abnormalities in multiple sclerosis. Magn Reson Med 44:583–591
2. Beaulieu C (2002) The basis of anisotropic water diffusion in the nervous system—a technical review. NMR Biomed 15:435–455
3. Beppu T, Nishimoto H, Ishigaki D, Fujiwara S, Yoshida T, Oikawa H, Kamada K, Sasaki M, Ogasawara K (2010) Assessment of damage to cerebral white matter fiber in the subacute phase after carbon monoxide poisoning using fractional anisotropy in diffusion tensor imaging. Neuroradiology 52:735–743
4. Chang KH, Han MH, Kim HS, Wie BA, Han MC (1992) Delayed encephalopathy after acute carbon monoxide intoxication: MR imaging features and distribution of cerebral white matter lesions. Radiology 184:117–122
5. Charlton RA, Barrick TR, McIntyre DJ, Shen Y, O'Sullivan M, Howe FA, Clark CA, Morris RG, Markus HS (2006) White matter damage on diffusion tensor imaging correlates with age-related cognitive decline. Neurology 66:217–222
6. Choi IS (1983) Delayed neurologic sequelae in carbon monoxide intoxication. Arch Neurol 40:433–435
7. Ernst A, Zibrak JD (1998) Carbon monoxide poisoning. N Engl J Med 339:1603–1608
8. Fan HC, Wang AC, Lo CP, Chang KP, Chen SJ (2009) Damage of cerebellar white matter due to carbon monoxide poisoning: a case report. Am J Emerg Med 27(757):e755–e757
9. Folstein MF, Folstein SE, McHugh PR (1975) "Mini-mental state". A practical method for grading the cognitive state of patients for the clinician. J Psychiatr Res 12:189–198
10. Fujiwara S, Beppu T, Nishimoto H, Sanjo K, Koeda A, Mori K, Kudo K, Sasaki M, Ogasawara K (2011) Detecting damaged regions of cerebral white matter in the subacute phase after carbon

monoxide poisoning using voxel-based analysis with diffusion tensor imaging. Neuroradiology. doi:10.1007/s00234-011-0958-8
11. Ide T, Kamijo Y (2008) Myelin basic protein in cerebrospinal fluid: a predictive marker of delayed encephalopathy from carbon monoxide poisoning. Am J Emerg Med 26:908–912
12. Jain K (2009) Carbon monoxide and other tissue poisons. In: Jain KK (ed) Textbook of hyperbaric medicine, 5th edn. Hogrefe and Huber Publisher, Massachusetts, pp 43–133
13. Kado H, Kimura H, Murata T, Itoh H, Shimosegawa E (2004) Carbon monoxide poisoning: two cases of assessment by magnetization transfer ratios and 1H-MRS for brain damage. Radiat Med 22:190–194
14. Kamijo Y, Soma K, Ide T (2007) Recurrent myelin basic protein elevation in cerebrospinal fluid as a predictive marker of delayed encephalopathy after carbon monoxide poisoning. Am J Emerg Med 25:483–485
15. Lapresle J, Fardeau M (1967) The central nervous system and carbon monoxide poisoning. II. Anatomical study of brain lesions following intoxication with carbon monixide (22 cases). Prog Brain Res 24:31–74
16. Lin WC, Lu CH, Lee YC, Wang HC, Lui CC, Cheng YF, Chang HW, Shih YT, Lin CP (2009) White matter damage in carbon monoxide intoxication assessed in vivo using diffusion tensor MR imaging. AJNR Am J Neuroradiol 30:1248–1255
17. Lo CP, Chen SY, Chou MC, Wang CY, Lee KW, Hsueh CJ, Chen CY, Huang KL, Huang GS (2007) Diffusion-tensor MR imaging for evaluation of the efficacy of hyperbaric oxygen therapy in patients with delayed neuropsychiatric syndrome caused by carbon monoxide inhalation. Eur J Neurol 14:777–782
18. O'Donnell P, Buxton PJ, Pitkin A, Jarvis LJ (2000) The magnetic resonance imaging appearances of the brain in acute carbon monoxide poisoning. Clin Radiol 55:273–280
19. Parkinson RB, Hopkins RO, Cleavinger HB, Weaver LK, Victoroff J, Foley JF, Bigler ED (2002) White matter hyperintensities and neuropsychological outcome following carbon monoxide poisoning. Neurology 58:1525–1532
20. Prockop LD, Chichkova RI (2007) Carbon monoxide intoxication: an updated review. J Neurol Sci 262:122–130
21. Shrout PE, Fleiss JL (1979) Intraclass correlations: uses in assessing rater reliability. Psychol Bull 86:420–428
22. Sohn YH, Jeong Y, Kim HS, Im JH, Kim JS (2000) The brain lesion responsible for parkinsonism after carbon monoxide poisoning. Arch Neurol 57:1214–1218
23. Terajima K, Igarashi H, Hirose M, Matsuzawa H, Nishizawa M, Nakada T (2008) Serial assessments of delayed encephalopathy after carbon monoxide poisoning using magnetic resonance spectroscopy and diffusion tensor imaging on 3.0T system. Eur Neurol 59:55–61
24. Thom SR (1990) Carbon monoxide-mediated brain lipid peroxidation in the rat. J Appl Physiol 68:997–1003
25. Thom SR, Bhopale VM, Fisher D, Zhang J, Gimotty P (2004) Delayed neuropathology after carbon monoxide poisoning is immune-mediated. Proc Natl Acad Sci USA 101:13660–13665
26. Thom SR, Bhopale VM, Han ST, Clark JM, Hardy KR (2006) Intravascular neutrophil activation due to carbon monoxide poisoning. Am J Respir Crit Care Med 174:1239–1248
27. Tievsky AL, Ptak T, Farkas J (1999) Investigation of apparent diffusion coefficient and diffusion tensor anisotrophy in acute and chronic multiple sclerosis lesions. AJNR Am J Neuroradiol 20:1491–1499
28. Uchino A, Hasuo K, Shida K, Matsumoto S, Yasumori K, Masuda K (1994) MRI of the brain in chronic carbon monoxide poisoning. Neuroradiology 36:399–401
29. Valk J, van der Knaap MS (1992) Toxic encephalopathy. AJNR Am J Neuroradiol 13:747–760
30. Vila JF, Meli FJ, Serqueira OE, Pisarello J, Lylyk P (2005) Diffusion tensor magnetic resonance imaging: a promising technique to characterize and track delayed encephalopathy after acute carbon monoxide poisoning. Undersea Hyperb Med 32:151–156
31. Weaver LK (2009) Clinical practice. Carbon monoxide poisoning. N Engl J Med 360:1217–1225
32. Weaver LK, Hopkins RO, Chan KJ, Churchill S, Elliott CG, Clemmer TP, Orme JF Jr, Thomas FO, Morris AH (2002) Hyperbaric oxygen for acute carbon monoxide poisoning. N Engl J Med 347:1057–1067
33. Weaver LK, Hopkins RO, Elliott G (1999) Carbon monoxide poisoning. N Engl J Med 340:1290 Author reply 1292
34. Zagami AS, Lethlean AK, Mellick R (1993) Delayed neurological deterioration following carbon monoxide poisoning: MRI findings. J Neurol 240:113–116
35. Zhang J, Piantadosi CA (1992) Mitochondrial oxidative stress after carbon monoxide hypoxia in the rat brain. J Clin Invest 90:1193–1199

Childs Nerv Syst
DOI 10.1007/s00381-012-1891-9

TECHNICAL NOTE

Use of magnetic resonance imaging to identify the edge of a dural tear in an infant with growing skull fracture: a case study

Hideki Matsuura · Shinichi Omama · Yuki Yoshida · Shunrou Fujiwara · Takayuki Honda · Manami Akasaka · Atsushi Kamei · Kuniaki Ogasawara

Received: 5 July 2012 / Accepted: 3 August 2012

Abstract
Purpose Growing skull fractures can be a challenging surgical problem facing pediatric neurosurgeons. The goal of this manuscript was to describe an effective surgical method used to treat a growing skull fracture.
Methods We present a case study of a 2-month-old boy who fell from his mother's arms and hit his head on the floor; he underwent X-ray, magnetic resonance (MR), and computed tomography (CT) imaging before cranioplasty with dural plasty.
Results X-ray performed on admission revealed a diastatic fracture with a gap of 8 mm in the right frontal bone and a linear fracture in the right occipital bone. X-ray performed 37 days after injury demonstrated that the gap had increased to 25 mm, and the patient was diagnosed with a growing skull fracture of the right parietal bone. Cranioplasty with dural plasty was performed on day 39. A combination of MR and CT images enabled the edge of the dural tear to be plotted on a three-dimensional image of the skull, and this was used to estimate the location of the edge of the dural tear on the scalp.
Conclusions We achieved excellent outcomes in terms of bony coverage and dural plasty. The combination of MR and CT images may be recommended for surgical repair of growing skull fracture in children.

Keywords Growing skull fracture · Enhanced MR imaging · Dural plasty · Cranioplasty

H. Matsuura (✉) · S. Fujiwara · K. Ogasawara
Department of Neurosurgery, Iwate Medical University,
Uchimaru 19-1,
Morioka 020-8505, Japan
e-mail: hidekima@iwate-med.ac.jp

S. Omama · Y. Yoshida
Department of Critical Care and Emergency Center,
Iwate Medical University,
Uchimaru 19-1,
Morioka 020-8505, Japan

T. Honda
Department of Plastic and Reconstructive Surgery,
Iwate Medical University,
Uchimaru 19-1,
Morioka 020-8505, Japan

M. Akasaka · A. Kamei
Department of Pediatrics, Iwate Medical University,
Uchimaru 19-1,
Morioka 020-8505, Japan

Introduction

Growing skull fractures are an uncommon complication of pediatric head trauma. The reported incidence of growing skull fractures ranges from 0.05 to 1.6 % [1]. The standard surgical treatment of the lesion involves repair of the dural defect with a graft and cranioplasty [3, 4]. The dural defect is usually larger than the bony defect; therefore, craniotomy around the fracture site is necessary, resulting in wider craniotomy [5]. Identifying the edge of the dural tear in presurgical planning may allow the area of the craniotomy to be minimized. The dura is enhanced by gadolinium on T1-weighted magnetic resonance (MR) images. Here, we describe a case of an infant with a growing skull fracture in which MR

Published online: 16 August 2012

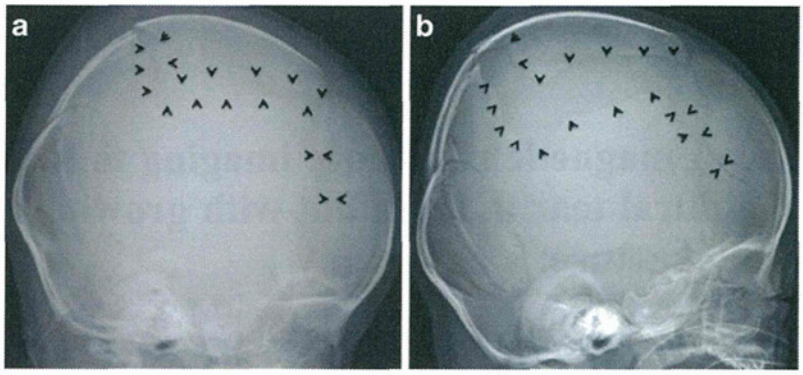

Fig. 1 **a** Lateral skull radiograph taken on initial presentation to hospital (day of accident). A diastatic right parietal skull fracture is evident, indicated by the *black arrowheads*. **b** Lateral skull radiograph taken 37 days after the accident. Enlargement of the fracture is evident, indicated by the *black arrowheads*

imaging with gadolinium enhancement was used to identify the edge of the dural tear. We use this case report to describe an effective surgical method for growing skull fractures.

Case report

A 2-month-old boy fell from his mother's arms and hit his head on the floor. Six hours later, he was transferred to our hospital. On admission, he presented with a small swelling in the right parietotemporal region. No consciousness disturbance or neurological deficits were observed. Plain cranial X-ray revealed a diastatic fracture with a gap of 8 mm in the right frontal bone and a linear fracture in the right occipital bone (Fig. 1a). Head computed tomography (CT) showed a thin subdural hematoma in the bilateral cerebral hemispheres. The patient's course was uneventful until the tenth day of hospitalization, when a bulge appeared in the right frontoparietal region. This bulge became progressively larger and firmer. Plain cranial X-ray performed 37 days after the onset of the head injury demonstrated that the bone defect had widened and the gap had increased to 25 mm (Fig. 1b). A CT scan revealed a leptomeningeal cyst herniating through the bone defect. Based on these findings, the patient was diagnosed with a growing skull fracture.

Prior to craniotomy to repair the lesion, the patient underwent MR imaging with gadolinium enhancement and three-dimensional CT. T1-weighted MR images showed the edge of the skull fracture as a discontinuity of the high-intensity signal from the bone marrow and the edge of the dural tear as discontinuity of gadolinium enhancement (Fig. 2). The distance between the edge of the skull fracture and the edge of the dural tear was measured on each slice, the thickness of which was 6.4 mm. The edge of the skull fracture identified on each MR image slice was identified on each corresponding CT image slice, and the edge of the dural tear was plotted on the reconstructed three-dimensional skull CT images based on the measurement from the MR images (Fig. 3).

After induction of general anesthesia, the edge of the growing skull fracture was identified on the scalp using manual palpitation, and the estimated edge of the dural tear was marked on the scalp using the reconstructed three-dimensional skull CT images (Fig. 4a). A skin incision was made, and the pericranial tissue corresponding to the area of the estimated edge of the dural tear was stripped. Craniotomy was performed with a margin of 1 cm for the estimated edge of the dural tear. The organized connective tissue was observed in the skull defect, and the spatial relation between craniotomy and the edge of the dural tear corresponded with the preoperatively estimated relation

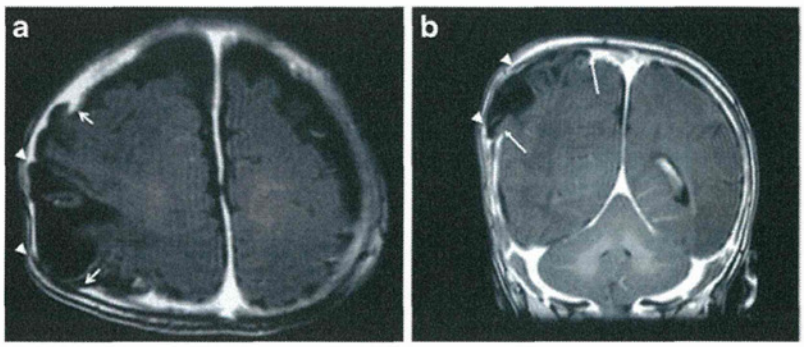

Fig. 2 **a** Axial enhanced T1-weighted MR image shows enhancement of dural tear (*arrow*) and the edge of skull fracture as discontinuity of high signal of the bone marrow (*arrow head*). **b** Coronal enhanced T1-weighted MR image shows enhancement of dural tear (*arrow*) and the edge of skull fracture as discontinuity of high signal of the bone marrow (*arrowhead*)

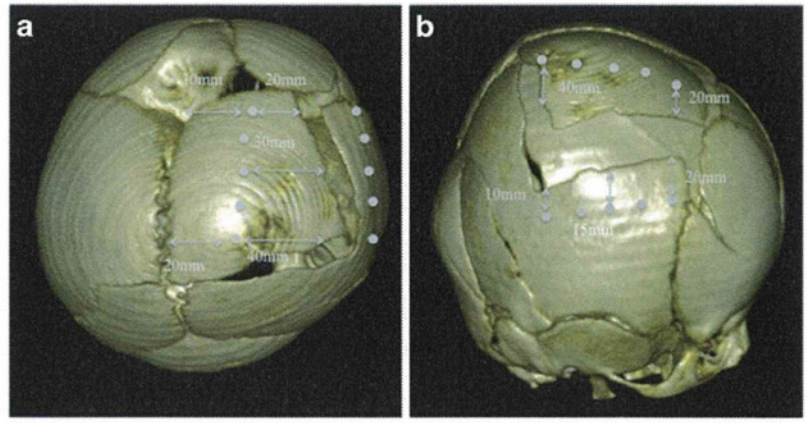

Fig. 3 Three-dimensional computed tomography images (**a**, **b**) showing distance measurements to the dural defect at the end of the bone

(Fig. 4b). The dural defect was covered with the stripped pericranial tissue (Fig. 4c), and cranioplasty was performed using the skull segmented on several pieces. The postoperative course was uneventful. A CT scan 1 year after surgery demonstrated a resolution of the growing skull fracture (Fig. 5).

Discussion

In the present case of a growing skull fracture, the edge of the skull fracture and the edge of the dural tear were identified from T1-weighted MR images [7]. This enabled the spatial relation between the two components to be identified. A combination of MR and CT images enabled the edge of the dural tear to be plotted on a three-dimensional image of the skull, and this was used to estimate the location of the edge of the dural tear on the scalp. As a result, the intraoperative spatial relation between craniotomy and the edge of the dural tear corresponded with the preoperatively estimated relation, and the area of the skin incision and craniotomy was minimized.

The autologous pericranial graft used in the repair of dural defects is histocompatible, less allergenic, well

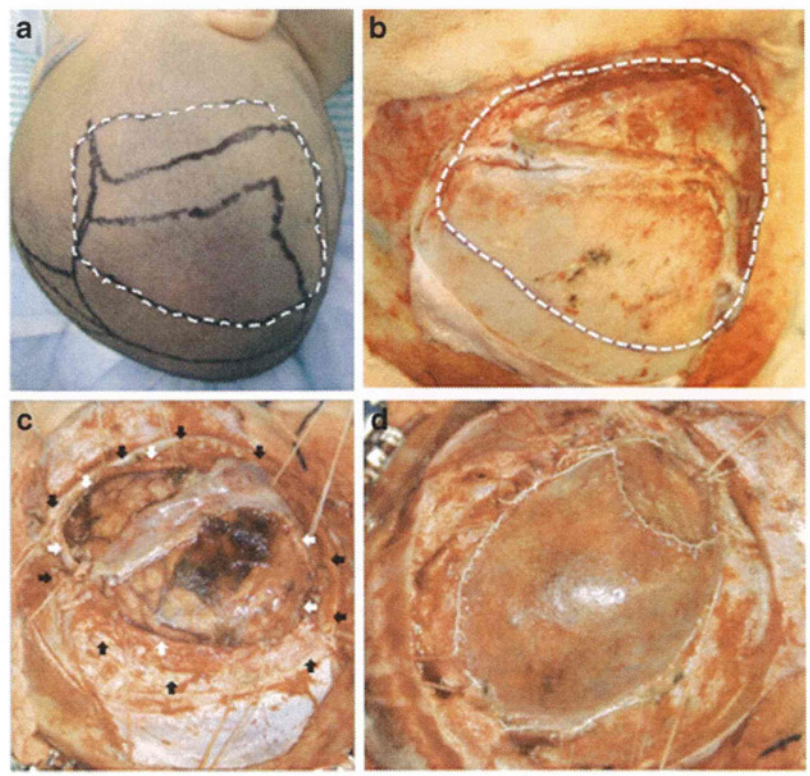

Fig. 4 **a** Photograph of the head of the patient prior to surgery. The *white dashed line* indicates the position of the dural defect over the temporal and parietal areas. **b** Photograph taken after the pericranial tissue had been dissected and the galeal tissue, adherent to the underlying bone defect. The *white dashed line* corresponds to the same area as in **c**. **c** Photograph taken after the galeal tissue adherent to the underlying bone defect and bone had been cut. *White arrows* indicate the outline of the dural defect. *Black arrows* indicate the bone flap margin. **d** Photograph showing the closure of the dural defect by pericranial graft

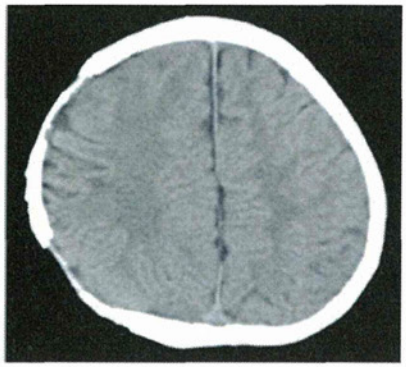

Fig. 5 Axial plain CT showing the expansion of the cerebral hemisphere and smooth bonding of the edge

vascularized and heals within the surrounding tissue [2]. In the present case, the pericranial graft was stripped in an area corresponding to the estimated edge of the dural tear, facilitating a minimal area of stripped pericranium.

In general, neuronavigation is used in an attempt to address growing skull fractures. However, children are less able than adults to tolerate the rigid head fixation required for the neuronavigation systems [6]. In particular, the use of a head clamp is inappropriate in children under 2 years of age [6]. The combination of MR and CT images may be recommended for surgical repair of growing skull fracture in children.

References

1. Arseni C, Civrea AV (1981) Clinicotherapeutic aspects in the growing skull fracture: a review of the literature. Childs Brain 8:161–172
2. Bashar A, Saffet T, Bulent C, Odhan Y, Banu T, Galip ZS (2009) Reconstruction of growing skull fracture with in situ galeal duraplasty and porous polyethylene sheet. J Craniofac Surg 20:1245–1249
3. Gupta SK, Reddy NM, Khosla VK, Mathuriya SN, Shama BS, Pathak A, Tewari MK, Kak VK (1997) Growing skull fractures: a clinical study of 41 patients. Acta Neurochir (Wine) 139:928–932
4. Halliday AC, Chapman PH, Heros RC (1990) Leptomeningeal cyst resulting from adulthood trauma: case report. Neurosurgery 26:150–153
5. Ziyal IM, Aydin Y, Turkmen CS, Salas E, Kaya AR, Ozveren F (1998) The natural history of late diagnosis or untreated growing skull fractures: report on two cases. Acta Neurochir (Wine) 140:651–654
6. Simon C, Mehapral S, Caroline H, Jothi K, Michael J, Maggie L, Conor M (2008) The use of noninvasive electromagnetic neuronavigation for slit ventricle syndrome and complex hydrocephalus in a pediatric population. J Neurosurg Pediatris 2:430–434
7. Vogler JB III, Murphy WA (1988) Bone marrow imaging. Radiology 168:679–693

Original Paper

Cerebrovascular Diseases

Cerebrovasc Dis 2012;34:358–367
DOI: 10.1159/000343505

Received: May 16, 2012
Accepted: September 14, 2012
Published online: November 14, 2012

Postoperative Cerebral White Matter Damage Associated with Cerebral Hyperperfusion and Cognitive Impairment after Carotid Endarterectomy: A Diffusion Tensor Magnetic Resonance Imaging Study

Takamasa Nanba[a, b] Kuniaki Ogasawara[b] Hideaki Nishimoto[a]
Shunrou Fujiwara[a] Hiroki Kuroda[c] Makoto Sasaki[a] Kohsuke Kudo[a]
Taro Suzuki[c] Masakazu Kobayashi[b] Kenji Yoshida[b] Akira Ogawa[b]

[a]Advanced Research Center, [b]Department of Neurosurgery and [c]Cyclotron Research Center, School of Medicine, Iwate Medical University, Morioka, Japan

Key Words
Carotid endarterectomy · Cerebral white matter · Hyperperfusion · Cognition

Abstract

Cerebral hyperperfusion after carotid endarterectomy (CEA), even when asymptomatic, often impairs cognitive function. However, conventional magnetic resonance (MR) imaging rarely demonstrates structural brain damage associated with postoperative cognitive impairment. MR diffusion tensor imaging (DTI) is potentially more sensitive for detection of white matter damage. Among the common parameters derived by DTI, fractional anisotropy (FA) is a marker of tract integrity, and mechanical disruption of axonal cylinders and loss of continuity of myelin sheaths may be responsible for reduced FA in white matter. The purpose of the present study was to determine whether postoperative cerebral white matter damage that can be detected by FA derived by DTI is associated with cerebral hyperperfusion after CEA and correlates with postoperative cognitive impairment. In 70 patients undergoing CEA for ipsilateral internal carotid artery stenosis (≥70%), cerebral blood flow (CBF) was measured using single-photon emission computed tomography (SPECT) before and immediately after CEA and on postoperative day 3. FA values in cerebral white matter were assessed using DTI before and 1 month after surgery. These values were normalized and analyzed using statistical parametric mapping 5. In each corresponding voxel in the pre- and postoperative normalized FA maps of each patient, a postoperative FA value minus a preoperative FA value was calculated, and a voxel with postoperatively reduced FA was defined based on data obtained from healthy volunteers. The number of voxels with postoperatively reduced FA was calculated and defined as the volume with postoperatively reduced FA. Neuropsychological testing, consisting of the Wechsler Adult Intelligence Scale Revised, the Wechsler Memory Scale and the Rey-Osterreith Complex Figure test, was also performed preoperatively and after the first postoperative month. Postoperative cognitive impairment on neuropsychological testing in each patient was defined based on data obtained from patients with asymptomatic unruptured cerebral aneurysms.
Post-CEA hyperperfusion on brain perfusion SPECT (CBF increase ≥100% compared with preoperative values) and postoperative cognitive impairment on neuropsychological testing were observed in 11 (16%) and 9 patients (13%), respectively. The volume with postoperatively reduced FA in

KARGER

Fax +41 61 306 12 34
E-Mail karger@karger.ch
www.karger.com

1015–9770/12/0346–0358$38.00/0

Accessible online at:
www.karger.com/ced

Kuniaki Ogasawara, MD
Department of Neurosurgery
Iwate Medical University
19-1 Uchimaru, Morioka 020-8505 (Japan)
E-Mail kuogasa@iwate-med.ac.jp

cerebral white matter ipsilateral to surgery was significantly greater in patients with post-CEA hyperperfusion than in those without ($p < 0.0001$). This volume in cerebral white matter ipsilateral to surgery was also significantly associated with postoperative cognitive impairment (95% confidence interval, 1.559–8.853; $p = 0.0085$). Cerebral hyperperfusion after CEA results in postoperative cerebral white matter damage that correlates with postoperative cognitive impairment.

Introduction

Cerebral hyperperfusion after carotid endarterectomy (CEA) is defined as a major increase in ipsilateral cerebral blood flow (CBF) after surgical repair of carotid stenosis that is well above the metabolic demands of the brain tissue [1, 2]. Cerebral hyperperfusion syndrome after CEA is characterized by unilateral headache, face and ocular pain, seizures, and focal symptoms related to cerebral edema or intracerebral hemorrhage [1–3]. Although the prognosis for patients with intracerebral hemorrhage is poor, the incidence is low (approx. 1%) [1–5]. Furthermore, neurological deficits in patients who develop cerebral hyperperfusion syndrome without experiencing subsequent intracranial hemorrhage tend to be reversible, as no major destruction of neural tissue due to intracranial hemorrhage occurs [5, 6]. By contrast, recent studies have demonstrated that the cerebral hyperperfusion phenomenon after CEA is often detected on CBF imaging and, even when asymptomatic, this phenomenon results in impairments of cognitive function [4, 6–8]. Such impairments may adversely affect quality of life [5, 8]. However, conventional magnetic resonance (MR) imaging, including diffusion-weighted imaging (DWI) and T2-weighted imaging, rarely demonstrates structural brain damage associated with postoperative cognitive impairment [7].

Another MR imaging technique, diffusion tensor imaging (DTI), is potentially more sensitive for detection of white matter damage [9]. DTI provides a quantitative, noninvasive method for delineating the anatomy of white matter pathways by measuring the magnitude and directionality of diffusion [10]. Among the common parameters derived by DTI, fractional anisotropy (FA) is a marker of tract integrity, and mechanical disruption of axonal cylinders and loss of continuity of myelin sheaths may be responsible for reduced FA in white matter [11]. FA shows stronger relationships with cognitive function than lesion volume displayed on conventional MR imaging in patients with age-related cognitive decline or cerebral small vessel disease [9, 12]. FA also correlates with cognitive function in chronic traumatic brain injury and Alzheimer's disease [13, 14].

The purpose of the present study was to determine whether postoperative cerebral white matter damage, which can be detected by FA derived by DTI, is associated with cerebral hyperperfusion after CEA and correlates with postoperative cognitive impairment.

Methods

Inclusion Criteria of Patients

Patients who were intended to undergo CEA and satisfied the following inclusion criteria were prospectively selected: age ≤75 years; ipsilateral cervical internal carotid artery (ICA) stenosis (≥70%); preoperative useful residual function (modified Rankin disability scale 0, 1 or 2); no ipsilateral carotid territory ischemic symptom before presentation to our department or ipsilateral carotid territory ischemic symptom that had occurred >2 weeks before presentation to our department; no massive cortical infarction confirmed by preoperative MR imaging using a 1.5-tesla imager (Signa MR/I; GE Healthcare, Milwaukee, Wisc., USA), including diffusion-weighted, T2-weighted and fluid-attenuated inversion recovery sequences, and obtaining written informed consent. Patients with new neurological deficits lasting for 2 weeks after surgery were excluded from the present study.

All study protocols were reviewed and approved by the institutional ethics committee.

CBF Measurements

CBF was assessed using [^{123}I]N-isopropyl-*p*-iodoamphetamine (IMP) and SPECT with a ring-type scanner (Headtome-SET 080; Shimadzu, Kyoto, Japan) before and immediately after CEA. In addition, patients with post-CEA hyperperfusion underwent a third CBF measurement in the same manner, 3 days after CEA. The IMP-SPECT study was performed as described previously [15], and CBF images were calculated according to the IMP autoradiography method [15, 16].

All SPECT images were transformed into standard brain size and shape by linear and nonlinear transformation using statistical parametric mapping (SPM) 99 software for anatomical standardization [17]. A 3-dimensional stereotaxic region-of-interest (ROI) template was used to automatically place 318 constant ROIs in both cerebral and cerebellar hemispheres [18]. ROIs were grouped into 10 segments (callosomarginal, pericallosal, precentral, central, parietal, angular, temporal, posterior, hippocampal and cerebellar) in each hemisphere according to the arterial supply. Eight (callosomarginal, pericallosal, precentral, central, parietal, angular, temporal, posterior) of these 10 segments were combined and defined as an ROI in the cortex of the cerebral hemisphere (fig. 1). Mean CBF was calculated in an ROI in the cerebral hemisphere ipsilateral to surgery before and after CEA. Post-CEA hyperperfusion was defined as a CBF increase of ≥100% (i.e. a doubling) compared with preoperative values, according to Piepgras et al. [1].

Intra- and Postoperative Management

All patients underwent surgery under general anesthesia. A continuous 8-channnel electroencephalography (EEG) tracing for detection of cerebral ischemia during ICA clamping was initiated after induction of anesthesia. No intraluminal shunt was used during ICA clamping in any patients. Mean duration of ICA clamping was 36 min (range, 28–48 min). In patients with post-CEA hyperperfusion, intensive control of arterial blood pressure between 100 and 140 mm Hg was instituted using intravenous administration of antihypertensive drugs immediately after SPECT. When CBF decreased and hyperperfusion resolved on postoperative day 3, pharmacological control of blood pressure was discontinued. However, when hyperperfusion persisted, systolic arterial blood pressure was maintained below 140 mm Hg. When hyperperfusion syndrome developed, the patient was placed in a propofol coma. A diagnosis of hyperperfusion syndrome required: (1) seizure, deterioration of level of consciousness, and/or development of focal neurological signs such as motor weakness, and (2) hyperperfusion on SPECT performed after CEA.

For detection of new intra- or postoperative lesions, all patients underwent T2-weighted and fluid-attenuated inversion recovery imaging and DWI using a 1.5-tesla whole-body imaging system within 7 days before and 1 day after surgery. Patients with cerebral hyperperfusion on CBF imaging performed immediately after surgery also underwent MR imaging on postoperative day 3 and after the first postoperative month. Furthermore, patients with cerebral hyperperfusion syndrome underwent additional MR imaging on the day on which symptoms developed. Two neuroradiologists (MS and KK) who were blinded to patient clinical information provided analysis of images and determined whether new lesions had developed postoperatively.

FA Measurements by DTI

DTI was performed using a 3.0-tesla superconductive MR imager with a gradient slew rate of 150 mT $m^{-1}ms^{-1}$ (Signa Excite HD; GE Healthcare) and an 8-channel head coil within 7 days before and 1 month after surgery. The following pulse sequences were used for DTI covering the entire brain: axial single-shot, spin-echo, echo-planar imaging (EPI); repetition time, 10,000 ms; echo time, 66 ms; 6 motion-probing gradient directions (b-value 1,000 s/m^2); matrix size, 128 128; field of view, 24 cm; slice thickness, 4.0 mm with 1.5-mm interslice gaps (voxel size, 1.9 1.9 4.0 mm); number of slices, 24; number of excitations, 3; parallel imaging reduction factor, 2, and acquisition time, 3 min 40 s.

For voxel-based analysis, we used SPM5 and original software developed with C/C++. SPM5 is freely available and distributed at the Wellcome Trust Centre for Neuroimaging web page (http://www.fil.ion.ucl.ac.uk/spm/), although this required MATLAB (The MathWorks, Natick, Mass., USA) as a software environment supplying numerous functions needed for image processing and statistical analysis in SPM5. For DTI voxel-based analysis, DTI parametric maps needed to be preprocessed using the techniques proposed in previous works [19, 20]. FA maps of each subject were masked using originally developed software with custom white matter masks, which were segmented using SPM5 from non-diffusion-weighted images (b = 0 s/mm^2). Using those masks, statistical analysis was performed only on voxels within the mask, and the effect of other tissues such as the gray matter and cerebrospinal fluid was decreased. As no templates of FA parametric maps were available in SPM5, the template was constructed from masked FA maps of 10 healthy subjects using the following method. First, the EPI template was used to normalize non-diffusion-weighted images and we applied the normalization parameter to the corresponding FA maps. Second, those normalized FA maps were smoothed with a 12-mm isotropic Gaussian kernel. Third, an averaged image of all smoothed FA maps of those subjects was defined as an FA template. Using the customized FA template, FA maps of each subject were again normalized. Finally, those normalized FA maps were smoothed with a 12-mm isotropic Gaussian kernel to improve the validity of statistical inferences and to reduce interindividual variation and coregistration errors.

In each corresponding voxel in the pre- and postoperative normalized FA maps of each patient, a postoperative FA value minus a preoperative FA value was calculated. As controls, 10 healthy volunteers (8 men; mean age, 33 years; range, 21–55 years) without any history of hypertension, diabetes mellitus, atrial fibrillation, pulmonary disease or presence of organic brain lesions, including

Fig. 1. Diagrams show the ROIs for a 3-dimensional stereotaxic ROI template for brain perfusion SPECT. White ROIs indicate the cerebral hemispheric cortex (callosomarginal, pericallosal, precentral, central, parietal, angular, temporal, posterior segments).

leukoaraiosis or asymptomatic lacunar infarction, on MR imaging underwent 2 separate DTI studies in the same manner. The interval between the two studies ranged from 1 month to 2 months. As a result, the mean – 2 SDs of the difference of the FA value (the second study value minus the first study value) was 0 to –0.05 in 26,664 voxels (24.9%), –0.05 to –0.10 in 60,683 voxels (56.6%), –0.10 to –0.15 in 17,425 voxels (16.2%), –0.15 to –0.20 in 2,381 voxels (2.2%) and –0.20 to –0.25 in 121 voxels (0.1%) from a total of 107,274 voxels in bilateral cerebral hemispheres. In each voxel in each patient, a difference of an FA value below the mean – 2 SDs of the value in the control group of healthy volunteers was defined as postoperatively reduced FA. In each cerebral hemisphere of each patient, the number of voxels with postoperatively reduced FA was calculated, and the ratio (%) of the number of voxels with postoperatively reduced FA to a total number of voxels of a unilateral cerebral hemisphere (53,637 voxels) was calculated and defined as the volume with postoperatively reduced FA.

Neuropsychological Evaluation

A battery of neuropsychological tests was administered, consisting of the Japanese translation of the Wechsler Adult Intelligence Scale Revised (WAIS-R) [21], the Japanese translation of the Wechsler Memory Scale [22], and the Rey-Osterreith Complex Figure test (Rey test) [23]. The WAIS-R provides measures of general intellectual function and generates a verbal and performance intelligence quotient (IQ). The Rey test evaluates copy and recall of a complex figure. As a result, 5 scores (WAIS-R verbal IQ; WAIS-R performance IQ; Wechsler Memory Scale; Rey copy and Rey recall) were used to evaluate cognitive function.

Neuropsychological tests were performed before and 1 month after surgery. All examinations were administered by a trained neuropsychologist who was blinded to the clinical information of patients.

As controls, 44 patients with asymptomatic unruptured cerebral aneurysms (17 men, 27 women; mean age, 56.8 years; range, 32–70 years) underwent the same neuropsychological tests before and 1 month after neck clipping by craniotomy [24]. None of the 44 patients had new postoperative neurological deficits or brain injury caused by surgery for aneurysms on postoperative computed tomography. Mean differences in each neuropsychological test score before and after neck clipping (postoperative scores – preoperative scores) were 2.4 4.6 in WAIS-R verbal IQ, 4.8 5.2 in WAIS-R performance IQ, 2.9 8.1 in the Wechsler Memory Scale, 0.2 1.1 in Rey copy, and 2.6 4.2 in Rey recall. As a result, the mean difference – 2 SD was –6.8 for WAIS-R verbal IQ, –5.6 for WAIS-R performance IQ, –13.3 for Wechsler Memory Scale, –2.0 for Rey copy and –5.8 for Rey recall. For the neuropsychological test scores of each patient undergoing CEA, a deficit was defined as a postoperative test score < preoperative score minus the absolute value of the mean – 2 SDs of the difference between the 2 test scores in the controls. A patient was considered as having postoperative cognitive impairment when one or more postoperative neuropsychological scores showed a deficit.

Statistical Analysis

Data are expressed as means SD. The relationship between each variable and the volume with postoperatively reduced FA in the cerebral white matter ipsilateral to surgery was evaluated using the Mann-Whitney U test. The relationship between each variable and postoperative cognitive impairment was evaluated by univariate analysis using the Mann-Whitney U test or χ^2 test. Multivariate statistical analysis of factors related to postoperative cognitive impairment was also performed using a logistic regression model. Variables with $p < 0.2$ in univariate analyses were selected for analysis in the final model. Differences were deemed statistically significant for values of $p < 0.05$.

Results

Over a period of 22 months, 70 patients satisfied the inclusion criteria. None of the patients developed new neurological deficits that lasted for 2 weeks after surgery. Thus, all 70 patients were analyzed in the present study.

The mean (SD) age of the patients (63 men, 7 women) was 67.9 7.6 years (range, 44–82). Concomitant disease states and symptoms were recorded, including hypertension in 62 patients, diabetes mellitus in 27 patients and hyperlipidemia in 36 patients. Fifty patients evidenced ipsilateral carotid territory symptoms, including 28 patients with transient ischemic attack, 8 patients with transient ischemic attack and subsequent stroke, and 14 patients with stroke alone. Twenty patients showed asymptomatic ICA stenosis. Preoperative MR imaging demonstrated infarction in the hemisphere ipsilateral to the ICA stenosis in 43 patients and no infarction in 27 patients. The contralateral ICA was occluded in 5 patients, and 12 additional patients showed 60–95% stenosis in the contralateral ICA. According to categories graded by Arnold et al. [25], 6 (9%) and 1 (1%) patients exhibited moderate and severe EEG changes during ICA clamping, respectively. DWI using a 1.5-tesla imager performed 1 day after surgery showed new hyperintense lesions only in the cerebral hemisphere ipsilateral to CEA in 9 of the 70 patients (13%) when compared with preoperative DWI. The diameter of all new hyperintense lesions was <1.0 cm.

Post-CEA hyperperfusion on SPECT was observed in 11 patients (16%). In 9 of these 11 patients, hyperperfusion had resolved in the SPECT performed on postoperative day 3, and pharmacological control of blood pressure was discontinued. These patients did not eventually develop new neurological symptoms. The remaining 2 patients with post-CEA hyperperfusion experienced a progressive increase in CBF on postoperative day 3 and developed hyperperfusion syndrome. One of these patients experienced motor weakness of the upper and lower extremities on the side contralateral to surgery on postoperative day 4. Another patient experienced focal seizures as evidenced by motor disturbances of the upper extremity on the side contralateral to surgery 5 days after surgery. Propofol coma was induced in these 2 patients. Af-

Table 1. Analysis of factors related to volume with postoperatively reduced FA

Variables	Volume with postoperatively reduced FA (mean SD), %		p value
Age			0.8416
≥70 years (n = 35)	3.1	4.6	
<70 years (n = 35)	2.3	2.1	
Gender			0.8987
Male (n = 63)	2.8	3.7	
Female (n = 7)	1.9	1.1	
Hypertension			0.2717
Yes (n = 62)	2.9	3.7	
No (n = 8)	1.5	1.3	
Diabetes mellitus			0.8848
Yes (n = 27)	2.4	2.3	
No (n = 43)	2.9	4.2	
Hyperlipidemia			0.5254
Yes (n = 36)	2.6	2.4	
No (n = 34)	2.8	4.5	
Symptomatic lesion			0.9896
Yes (n = 50)	2.7	3.9	
No (n = 20)	2.6	2.7	
Infarction on preoperative MR imaging			0.6903
Yes (n = 43)	2.8	4.2	
No (n = 27)	2.5	2.3	
Bilateral lesions			0.9781
Yes (n = 17)	2.6	4.0	
No (n = 53)	2.7	3.5	
Duration of ICA clamping			0.6915
≥40 min (n = 19)	2.3	1.9	
<40 min (n = 51)	2.9	4.0	
EEG changes during ICA clamping			0.3370
Yes (n = 7)	5.0	7.2	
No (n = 63)	2.5	2.9	
New ischemic lesions on DWI on postoperative day 1			0.8126
Yes (n = 9)	3.6	6.6	
No (n = 61)	2.6	2.9	
Postoperative hyperperfusion			<0.0001
Yes (n = 11)	8.1	6.0	
No (n = 59)	1.7	1.5	

Table 2. Univariate analysis of factors related to postoperative cognitive impairment

Variables	Postoperative cognitive impairment				p value
	yes (n = 9)		no (n = 61)		
Age, years	67.0	5.0	67.8	7.9	0.4553
Male gender	9 (100)		54 (89)		0.5831
Hypertension	9 (100)		53 (87)		0.5841
Diabetes mellitus	4 (44)		23 (38)		0.7258
Hyperlipidemia	6 (67)		30 (49)		0.4791
Symptomatic lesion	6 (67)		44 (72)		0.7082
Infarction on preoperative MR imaging	6 (67)		37 (61)		>0.9999
Bilateral lesions	1 (11)		16 (26)		0.4376
Duration of ICA clamping, min	35.1	6.6	37.0	5.4	0.3121
EEG changes during ICA clamping	1 (11)		6 (10)		>0.9999
New ischemic lesions on DWI on postoperative day 1	1 (11)		8 (13)		>0.9999
Postoperative hyperperfusion	6 (67)		5 (8)		0.0002
Volume with postoperatively reduced FA, %	9.8	5.7	1.6	1.3	<0.0001

Values are means SD or numbers with percentages in parentheses.

ter termination of the propofol coma, these patients eventually experienced full recovery. None of the 11 patients with post-CEA hyperperfusion exhibited new lesions on MR imaging using a 1.5-tesla imager performed on postoperative day 3, the day on which symptoms developed, or after the first postoperative month.

Among the 70 patients studied, the volume with postoperatively reduced FA ranged from 0.1 to 21.0% (mean, 2.7 3.6) in the cerebral hemisphere ipsilateral to surgery and from 0.1 to 5.4% (mean, 1.9 1.4) in the contralateral cerebral hemisphere. Results of analysis of factors related to the volume with postoperatively reduced FA in the cerebral hemisphere ipsilateral to surgery are summarized in table 1. This volume was significantly greater in patients with post-CEA hyperperfusion than in patients without. No other variables were significantly associated with the volume showing postoperatively reduced FA.

At postoperative neuropsychological assessment, 9 patients (13%) showed postoperative cognitive impairment. Results of univariate analysis of factors related to postoperative cognitive impairment are summarized in table 2. The incidence of post-CEA hyperperfusion was significantly higher in patients with postoperative cognitive impairment than in those without. The volume with postoperatively reduced FA in the cerebral hemisphere ipsilateral to surgery was significantly greater in patients with postoperative cognitive impairment than in those without. Figure 2 shows relationships among volumes with postoperatively reduced FA in the cerebral hemisphere ipsilateral to surgery, post-CEA hyperperfusion and postoperative cognitive impairment. Other variables were not significantly associated with postoperative cognitive impairment. After eliminating variables that were closely re-

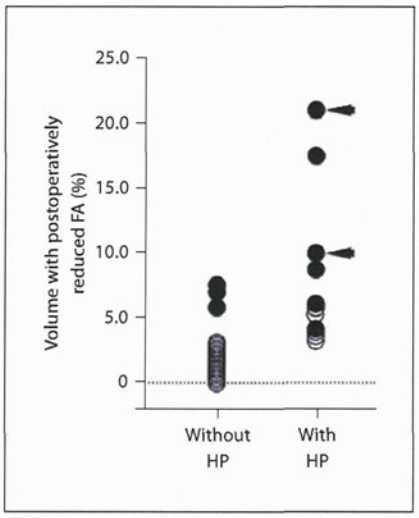

Fig. 2. Relationship between volume with postoperatively reduced FA in the cerebral white matter ipsilateral to surgery, postoperative hyperperfusion (HP) and postoperative cognitive impairment. The volume was significantly greater in patients with postoperative hyperperfusion than in those without ($p < 0.0001$) and was significantly greater in patients with postoperative cognitive impairment than in those without ($p < 0.0001$). Closed and open circles indicate patients with and without postoperative cognitive impairment, respectively. Arrows indicate patients with cerebral hyperperfusion syndrome.

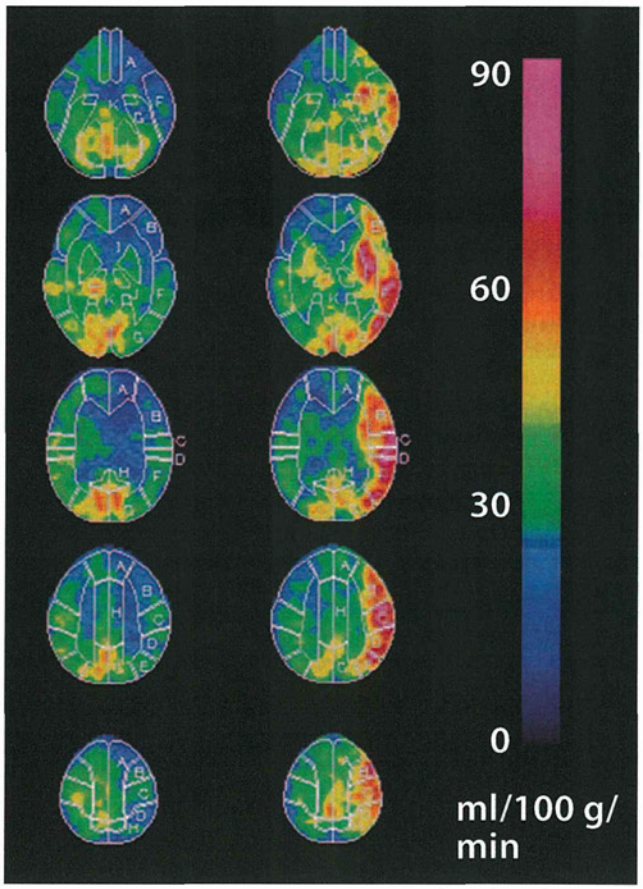

Fig. 3. A 73-year-old man with symptomatic left ICA stenosis (90%) exhibiting cerebral hyperperfusion syndrome and cognitive impairment after left CEA. Preoperative brain perfusion SPECT shows reduced blood flow in the left hemisphere (left row) where hyperperfusion develops immediately after surgery (right row).

lated to others, the following items with values of $p < 0.2$ in univariate analyses were adopted as confounders in the logistic regression model for multivariate analysis: post-CEA hyperperfusion; and volume with postoperatively reduced FA in the cerebral hemisphere ipsilateral to surgery. This analysis revealed that volume with postoperatively reduced FA in the cerebral hemisphere ipsilateral to surgery was significantly associated with postoperative cognitive impairment (95% confidence interval, 1.559–8.853; $p = 0.0085$). Figures 3 and 4 show SPECT and MR images, respectively, in a patient with cerebral hyperperfusion syndrome and cognitive impairment after surgery.

Discussion

Previous studies have demonstrated that patients with asymptomatic cerebral hyperperfusion on CBF imaging do not exhibit new postoperative lesions on conventional MR imaging and that even reversible vasogenic or cytotoxic edema on MR imaging develops in less than half of patients with cerebral hyperperfusion syndrome [7, 26]. This is consistent with results from the present study.

Post-CEA hyperperfusion often develops in the cerebral hemisphere ipsilateral to surgery, but not in the contralateral cerebral cortex [6]. The present study therefore evaluated the volume with postoperatively reduced FA only in the ipsilateral cerebral white matter. As a result, the volume was significantly greater in patients with post-CEA hyperperfusion than in those without. These data suggest that cerebral hyperperfusion after CEA results in postoperative white matter damage.

Postoperative white matter damage may also occur through other mechanisms. For example, a significant number of patients display evidence of gaseous or par-